Circulation and Scale-Up in Bubble Columns

Nicholas W. Geary and Richard G. Rice
Dept. of Chemical Engineering, Louisiana State University, Baton Rouge, LA 70803

The liquid circulation model of Rice and Geary (1990) is extended to include turbulence originating at the wall. Thus, two possible length scales are considered: one originating from rising bubbles and the other emanating from the wall. The appropriate scale for small columns should be based on bubble size, while for larger systems the proper mixing length is proportional to column diameter. It is proposed that the film Reynolds number may be the key in distinguishing the two cases.

Introduction

Paralleling the recent advances in biotechnology is the increased use of bubble columns. It is thus important that techniques be made available to calculate the effect of scale-up on liquid mixing in such columns. At the most fundamental level, this requires information regarding the local liquid velocity profiles. Recently (Clark et al., 1987; Rice and Geary, 1990), success was reported using the separated-flow model to predict velocity. This approach begins with the following momentum balances (Ishii, 1975; Ishii and Zuber, 1979; Rietema, 1982):

$$(1-\epsilon)\rho_c U_c \frac{\partial U_c}{\partial z} = -\nabla\cdot(1-\epsilon)T_c - (1-\epsilon)\nabla p - (1-\epsilon)\rho_c g + F_s \quad (1)$$

$$\epsilon\rho_d U_d \frac{\partial U_d}{\partial z} = -\nabla\cdot\epsilon T_c - \epsilon\nabla p - \epsilon\rho_d g - F_s \quad (2)$$

where F_s is the "slip force" or interfacial drag force per unit volume, and the local voidage is taken to depend only on radial position so that $\epsilon = f(r)$. In this analysis, the liquid sustains both viscous stress, τ_c, and Reynolds stress, R_c, such that $T_c = \tau_c + R_c$. This treatment differs from that of Rietema (1982) who did not include liquid Reynolds stresses acting on the gas phase. Bubble-bubble interactions are ignored, but the total stress T_c is taken to act uniformly on the whole. If phase densities are constant throughout, continuity relations will require the lefthand sides of both momentum equations to be identically zero. The proposed separated flow equations should, when added, yield the correct homogeneous-phase result. This necessary condition is obeyed by the above relations which combine to yield:

$$0 = -\nabla\cdot T_c - \nabla p - \bar{\rho}g \quad (3)$$

To successfully compute mixing times from the proposed model, it is essential that the hypothesis of one main recirculation zone be correct. Joshi and Sharma (1979) proposed that multiple circulation cells of height equal to the column diameter exist. Recently, however, Devanathan et al. (1990) were able to measure experimentally liquid velocities throughout an entire column (using radioactive tracers) and concluded that only two cells existed, the largest of which encompasses nearly the whole column. In the lower cell (which was confined to the entry region), the liquid was determined to ascend at the wall and descend at the column center. In the upper cell (which occupied the rest of the column), this pattern was reversed.

This recent evidence gives support to the approach used by Rice and Geary (1990) and Clark et al. (1987), in which liquid circulation was described as boyancy-driven and resulted from a radial voidage profile. In terms of a dimensionless radius ($\xi = r/R$), the voidage profile was modeled by Rice and Geary (1990) as two distinct zones:

$$\epsilon(\xi) = \bar{\epsilon}\left(\frac{m+2}{m}\right)\frac{1}{\lambda^2}\left[1-\left(\frac{\xi}{\lambda}\right)^m\right];\ \xi \le \lambda$$

$$\epsilon(\xi) = 0;\ \xi \ge \lambda \quad (4)$$

The exponent m is normally fitted using local voidage data. Note, as it is implied in the above, that there exists a thin downflowing (bubble-free) layer near the wall, the maximum downflowing velocity position being λ. The substitution of the above distribution into Eqs. 1 and 2, followed by direct integration, yielded the stress relations:

Correspondence concerning this article should be addressed to R. G. Rice.

$$T_c(\xi) = \frac{\rho_c g R}{2}\left(\frac{2\bar{\epsilon}}{m\lambda^2}\right)\xi\left[1-\left(\frac{\xi}{\lambda}\right)^m\right];\ \xi \le \lambda \tag{5}$$

$$T_c^*(\xi) = \frac{\rho_c g R}{2}\left(\frac{\bar{\epsilon}}{\lambda^2}\right)\left(\frac{\lambda^2-\xi^2}{\xi}\right);\ \xi \ge \lambda \tag{6}$$

where the flux continuity conditions have been used: $T_c(0)=0$ and $T_c(\lambda)=T_c^*(\lambda)=0$.

Closure Relations

In the original analysis by Rice and Geary (1990), the integration for velocity profiles was completed using a strain model that incorporated both viscous and Reynolds stresses. The latter was confined to the bubbly core ($0 \le \xi \le \lambda$) where it was proposed that the Reynolds stress obeyed Prandtl's model with a locally varying mixing length, $\ell(\xi)$. The fluid in the wall vicinity was assumed to undergo viscous, laminar flow. In large columns, it is likely that the downflowing wall region will also sustain turbulence, as suggested by Anderson and Rice (1989). This modification is significant especially if some fraction of the core eddies are generated at the wall, as for single-phase flow.

The original closure relationships are therefore modified to account for turbulence in the wall region. Thus, for both core and wall regions, we combine the viscous and Reynolds stresses:

$$\frac{\mu_c}{R}\left(-\frac{\partial U_c}{\partial \xi}\right) + \rho_c\frac{\ell^2(\xi)}{R^2}\left(-\frac{\partial U_c}{\partial \xi}\right)^2 = T_c(\xi),\ 0<\xi\le\lambda \tag{7}$$

$$-\frac{\mu_c}{R}\left(\frac{\partial U_c^*}{\partial \xi}\right) - \frac{\rho_c[\ell^*(\xi)]^2}{R^2}\left(\frac{\partial U_c^*}{\partial \xi}\right)^2 = T_c^*(\xi),\ \lambda<\xi\le 1 \tag{8}$$

Quantities with asterisk denote the wall region.

Mixing Length Scale

The choice of a correct mixing length scale for the core fluid has been debated recently. Clark et al. (1987) and Devanathan et al. (1990) recommend the use of a single-phase length scale as measured by Nikuradse (from Schlichting, 1960). In contradiction to this, Rice and Geary (1990) and Geary and Rice (1991) argue that the proposed mixing length scale should be made proportional to the bubble size. Such an approach could be based on the premise that the vortices produced in the wake of a bubble would suppress the latent turbulence arising at the wall from liquid circulation and would therefore dominate local mixing.

In many cases, the predictions based on either of the two length scale models are so similar (each with some experimental support) that discrimination between the two proposals is yet unclear. Cohen (1991) measured the effect of holdup on stirrer-generated turbulence (in liquid-liquid dispersions) and determined that turbulence damping increased with holdup. This suggests that bubbles interfere with latent turbulence, implying that both sources of eddy formation may be significant.

Support for a bubble-based mixing scale can be found in the publications of Lubbert and coworkers (Lubbert et al., 1990; Lubbert and Larson, 1990) who undertook to determine the origin of multiphase turbulence. In their work, heat tracers were used to measure the degree of dispersion that occurred over small distances within a bubble column. By considering the standard deviation of the measured signal, Lubbert concluded that not only was the turbulence nonisotropic, but that the dominant mixing mechanism arises from bubble wakes. Moreover, they noted that "the rising bubbles suppressed the development of the long cascade of stochastical eddies, which is a necessary condition to maintain local isotropic turbulence."

Incorporating these observations into a general relationship for the mixing lengths requires examination of a turbulent wall region, which thus gives rise to at least two core mixing lengths: one bubble-induced and the other originating at the wall and propagating into the core (as in single-phase flow). For the core, mechanical energy dissipation is minimal when mixing length is the largest, so we propose:

$$\ell = \mathrm{Max}(\ell_B, \ell^*),\ 0<\xi\le\lambda \tag{9}$$

where ℓ^* represents the wall-induced mixing scale and ℓ_B the bubble generated scale. In the region of the wall, turbulent eddies can be generated only from boundary layer instabilities. The behavior of the liquid phase (which is bubble-free in this region) can be considered analogous to single-phase pipe flow, for which Nikuradse experimentally determined the following mixing length scale:

$$\ell^* = R(0.14 - 0.08\ \xi^2 - 0.06\ \xi^4) \tag{10}$$

which is proportional to column diameter. This well-known result describes the manner by which turbulent eddies, generated at the wall, propagate away from the boundary. In the two-phase analysis, consideration must also be given to turbulence arising from the movement of bubbles. This scale, based naturally on bubble size and population density, was modified recently (Geary and Rice, 1991) to account for deformed, ellipsoidal-shaped bubbles:

$$\ell_B = (d/\alpha^{1/3})\cdot\epsilon(\xi)/\bar{\epsilon} \tag{11}$$

where α is a bubble-shape correction factor.

Wall Region Mixing Length Scale

The single-phase mixing scale, originating in the wall region, can propagate into the core, where there can exist eddies generated from different sources, namely wall- and bubble-induced. Their interaction is a complex phenomenon, which is not well documented. However, a simple energy minimization criteria (discussed later) can be applied. Equation 9 governs the extent to which the continuous single-phase scale (Eq. 10) is applicable. The consequence of introducing a turbulent wall region to the model is illustrated in Figure 1. By equating Eqs. 5 and 7 and Eqs. 6 and 8, followed by direct integration, the velocities $U_c(\xi)$ and $U_c^*(\xi)$ can be found as before in the manner of Rice and Geary (1990). In Figure 1, we compare this earlier prediction (using a purely viscous condition at the wall) with predictions including wall turbulence, using Hills' (1974) experiments for reference. At the wall, the velocity gradient is considerably smoother than the rather sharp profiles of earlier models (Rice and Geary, 1990; Clark et al., 1987; Walter, 1983), where the inset illustrates computations for a purely viscous wall condition.

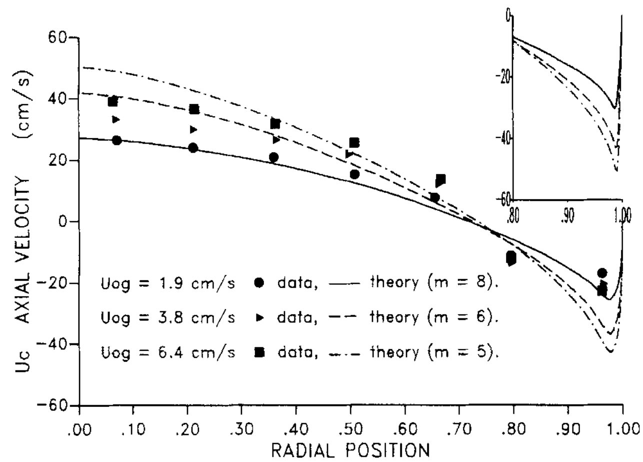

Figure 1. Effect of adding Reynolds stresses to down-flowing liquid: comparison with Hills' (1974) Data.

Inset depicts laminar results.

In Figure 2, we demonstrate the application of Eq. 9 and show that the local length scale is either the local value of mixing length using the original Rice-Geary (1990) model ($\ell \propto d$) or the equivalent single-phase scale, $\ell^*(\xi)$. This figure, which serves to demonstrate the method by which the heretofore separate models are combined, represents the length scale used for Hills' (1974) column (U_{og} = 3.8 cm/s); it therefore complements Figure 1. It is clear that these scales are very nearly the same size. This is not altogether unexpected, considering the results of Clark et al. (1987) compared to Rice and Geary (1990), the former using only a latent turbulence model and the latter using solely a bubble-based scale.

Mixing Length Based on Bubble Size

In Eq. 11, the eddy size is written to include a correction factor ($\alpha^{1/3}$) to account for deformation. The aspect ratio, α, represents the height to breadth ratio of an ellipsoidal bubble. This is necessary since the size of eddies formed behind bubbles will be proportional to the major axis (Fan and Tsuchiya, 1990), as discussed recently by Geary and Rice (1991). The implied dependence of turbulence length scale on eddy width is consistent with Prandtl's original hypothesis which required that "the mixing length (ℓ) be proportional to the width of the turbulent mixing zone" (Hinze, 1975).

Core Turbulence with Origins at the Wall

The single-phase mixing length $\ell^*(\xi)$ relationship was based on the data of Nikuradse who found that ℓ^* was independent of the Reynolds number when this exceeded 1.1×10^5. This may explain why small columns and higher viscosity solutions tend to be dominated by bubble-generated turbulence (Cristi et al., 1988; Lubbert and Larson, 1990) since the appropriate Reynolds number is too small to precipitate wall-induced turbulence. For industrial applications, however, Eq. 10 may more accurately reflect the true situation. Under such circumstances, the bubble size has little effect on the intensity of liquid mixing. In the following section, a criterion is developed that delineates the applicable operating region for each model.

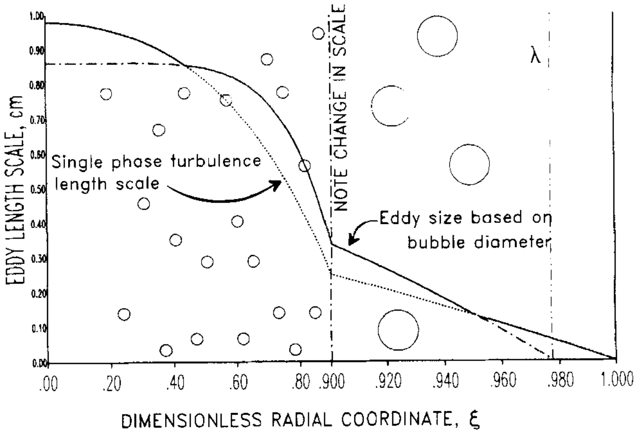

Figure 2. Eddy length scale variation for Hills' (1974) column (U_{og} = 3.8 cm/s).

Energy Minimization

The final aspect of the new model is the manner by which the two possible length scales are incorporated. Choosing the maximum denoted in Eq. 9 reflects the principle of energy minimization, apparently first used for viscous flow by Rietema and Ottengraf (1970). The equation for overall rate of mechanical energy dissipation can be written (Ishii, 1975) in terms of Reynolds stresses:

$$E_m = \int_V -U_c \cdot \nabla \cdot (1-\epsilon) R_c dV \tag{12}$$

which is rearranged to yield:

$$E_m = \int_V \left\{ -\nabla \cdot [(1-\epsilon) R_c \cdot U_c] + (1-\epsilon) R_c : \nabla U_c \right\} dV \tag{13}$$

When integrated, the first group of terms contribute nothing [since $U_c(1) = 0$ and $R_c(0) = 0$], thus the energy dissipation can be expressed for one-dimensional flow as:

$$E_m = \int_V \left\{ (1-\epsilon(\xi)) R_c(\xi) \frac{\partial U_c}{\partial \xi} \right\} dV \tag{14}$$

where $R_c(\xi)$ is the local Reynolds stress. This shows that energy dissipation is inversely proportional to either d (bubble-induced turbulence) or R (wall-induced turbulence). The minimum energy is sustained for the largest of these two possible scales.

Tests of New Theory

By inserting the closure relations (Eqs. 7 and 8) into Eqs. 5 and 6, we find:

$$\frac{dU_c}{d\xi} = \frac{\nu_c R}{2\ell^2(\xi)} \left[1 - \sqrt{1 + \frac{2gR\ell^2(\xi)}{\nu_c^2} \cdot \beta(\xi)} \right] = F_c(\xi, \ell) \tag{15}$$

$$\frac{dU_c^*}{d\xi} = \frac{\nu_c R}{2[\ell^*(\xi)]^2} \left[1 - \sqrt{1 + \frac{2gR\ell^{*2}(\xi)}{\nu_c^2} \cdot \gamma(\xi)} \right] = F_c^*(\xi, \ell^*) \tag{16}$$

where $\ell(\xi)$ and $\ell^*(\xi)$ are given in Eqs. 9 and 10, and the definitions of $\beta(\xi)$ and $\gamma(\xi)$ are:

$$\beta(\xi)=\frac{2\bar{\epsilon}}{m\lambda^2}\,\xi\left[1-\left(\frac{\xi}{\lambda}\right)^m\right] \tag{15a}$$

$$\gamma(\xi)=\frac{\bar{\epsilon}}{\lambda^2}\left(\frac{\xi^2-\lambda^2}{\xi}\right) \tag{16a}$$

Integration of Eqs. 15 and 16 yields:

$$U_c(\xi)-U_c(0)=\int_0^{\xi}F_c d\xi \tag{17}$$

$$U_c^*(\xi)-U_c(\lambda)=\int_{\lambda}^{\xi}F_c^* d\xi \tag{18}$$

Since $U_c^*(1)=0$, and $U_c(\lambda)=U_c^*(\lambda)$, it is easy to see that the centerline velocity is:

$$U_c(0)=-\left[\int_0^{\lambda}F_c d\xi+\int_{\lambda}^{1}F_c^* d\xi\right] \tag{19}$$

The only remaining unknown, λ, is determined through the use of the conservation equation for batch flow. This requires upflow to equal downflow (Rice and Geary, 1990):

$$0=-\frac{1}{2}\int_{\lambda}^{1}\frac{\partial U_c^*}{\partial \xi}\,\xi^2 d\xi-\frac{1}{2}\int_0^{\lambda}\frac{\partial U_c}{\partial \xi}\,\xi^2 d\xi$$
$$+\frac{1}{2}\bar{\epsilon}\cdot\left(\frac{m+2}{m\lambda^2}\right)\int_0^{\lambda}\frac{\partial U_c}{\partial \xi}\,\xi^2\left[1-\frac{2}{m+2}\cdot\left(\frac{\xi}{\lambda}\right)^m\right]d\xi$$
$$-\frac{1}{2}\bar{\epsilon}U_c^*(\lambda) \tag{20}$$

The consequences of introducing turbulence to the wall region have already been illustrated (Figure 1). The model seemed to track the small-column data of Hills (1974) reasonably well, without predicting unreasonably sharp profile shapes.

Additional evidence to support the theory requires comparisons with a wider range of circumstances. Two examples are presented. In these examples, the length scale is chosen according to the criterion given in Eq. 9. In the first, the bubble scale dominates, while in the second, the single-phase Nikuradse scale is seen to take over.

Devanathan et al. (1990) measured mean and fluctuating liquid velocities, from which Reynolds stresses were calculated. Their final results (mean velocity and local eddy viscosity) are compared to those of the present model in Figures 3*a* and 3*c*, inspection of which shows clearly that bubble size is the principal scale (Figure 3b). The agreement obtained with these separate measurements is remarkable, given that the bubble size used was determined from a simple visual observation (Devanathan, 1990). Also plotted in Figure 3a is the predicted liquid velocity profile, if the mixing length scale was taken to be $\ell^*(\xi)$ throughout (Eq. 10). It is clear from Figure 3b that the scale ℓ^* is too small and would thus cause significant overestimates of velocity.

Experiments on large columns are quite sparse in the literature. Perhaps the most complete are the related works of Kojima et al. (1980) and Koide et al. (1979). In these articles, both voidage and velocity profiles are reported. The voidage data are fitted with a power-law equation, similar to Eq. 4, and this fit is illustrated in Figure 4a. The exponent m takes a value around 100; this, of course, implies very flat voidage profiles, a condition (Rice and Geary, 1990) known to minimize circulation. Even for this extreme case, the comparison with our model (Figure 4c) is again quite good. Considering Figure 4b, it is clear that the correct mixing length is given by $\ell^*(\xi)$ almost throughout (Eq. 10). A mixing scale based on the bubble size overpredicts measured velocity, although again ℓ_B and ℓ^* are within an order of magnitude (Figure 4b). Thus, it may be argued that wall turbulence affects bubble interaction, thereby influencing the rates of coalescence and breakage, and equilibrium bubble size (Prince and Blanch, 1990).

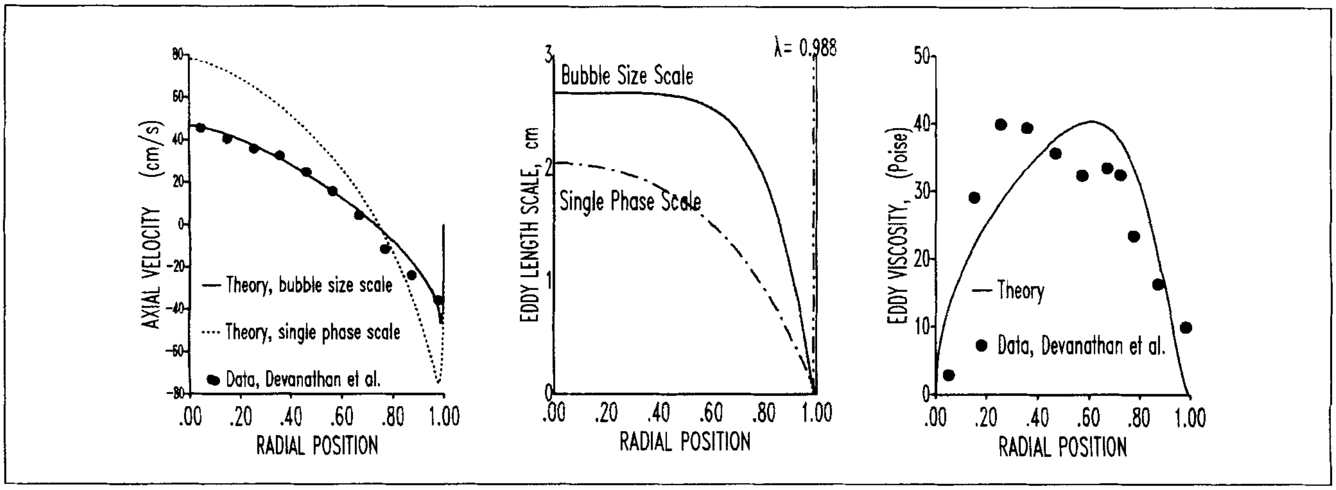

Figure 3. Small-column comparison of theory with data of Devanathan et al., (1990): a) liquid velocity profile: b) applicable eddy length scale; c) eddy viscosity.

Data for superficial gas velocity of 10.5 cm/s, $\bar{\epsilon}=0.18$, $d=1.5$ cm, $\alpha=0.415$, $m=6$ (optimized). The zero velocity point was experimentally found to be 0.72 (theory = 0.726).

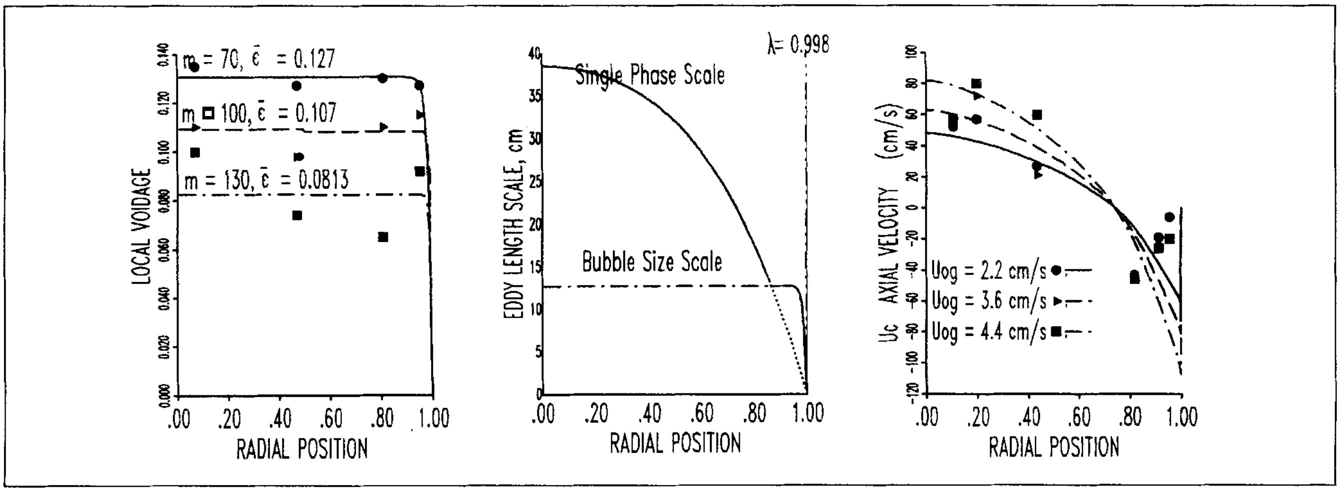

Figure 4. Large-column comparison with data of Koide et al. (1979) and Kojima et al. (1980): a) voidage profile: b) applicable eddy length scale; c) velocity profile.

Scale-Up Predictions

Mixing times rely primarily on the liquid circulation velocity, U_c. The theory derived herein can thus be used to predict the dependencies of mixing time on experimental conditions. The results obtained (Eqs. 17 and 18) suggest a square-root dependence of the mixing time on gas holdup. The theory also predicts very weak dependence on either liquid ($\mu_c < 1$ Pa·s) or gas properties. Secondary effects will result from the way these properties influence the bubble size (hence turbulence length scale), voidage and voidage profile (see for instance Shah et al., 1982). The liquid velocities are not affected strongly by a viscosity change, except in the region close to the wall where an increase in solution viscosity decreases λ, leading to a thicker wall layer. We can therefore conclude that liquid properties have very little effect on mixing times. This was experimentally confirmed by Yoshitome and Shirai (1970), who reported only a weak dependence of liquid velocity on both surface tension and liquid viscosity.

The impact of column diameter cannot accurately be considered without due regard to the local turbulence length scale and voidage profiles. The approximate scale-up predictions (based on the current theory) for column diameter and other important parameters can be summarized:

$$\tau_{\text{mix}} \propto \epsilon^{0.5} \mu^0 \sigma^0 D_c^{n+0.5} \tag{21}$$

where n is unity for small columns and zero for large. It is also noted that the superficial gas velocity may be incorporated into Eq. 21 using suitable correlations (such as drift-flux) to relate voidage to velocity. This possibility is explored in Table 1, where the scale-up predictions are summarized. The exponents are generally smaller for experimental data than forecast by present theory.

Comments and Conclusions

The original circulation model of Rice and Geary (1990) has been extended to include the possibility of natural turbulence originating at the wall. This scale is compared with the scale of turbulence originating from the rising bubbles. A simple local energy minimization approach is utilized which allowed the liquid circulation and eddy viscosity to be estimated for a

Table 1. Mixing Time Scale-Up Predictions

Parameter	Pred. Exponent	Lit. Exponent	Comments
ϵ (Voidage)	$\frac{1}{2}$	~0.26	Correlation by Ulbrecht et al. (1985)
U_{o_g} (Superficial Gas Vel.)	$\frac{1}{2}$ *	0.5 0.5	Correlation by Ulbrecht et al. (1985) Correlation by Wisecarver et al. (1990)
μ_c (Viscosity)	0**	~0	Yoshitome and Shirai, 1970 found no significant effect of surface tension or liquid viscosity on $U_c(0)$
σ (Surface Tension)	0	~0	
D_c (Column dia.)	$\frac{3}{2}$ † (Small Col.)	—	
	$\frac{1}{2}$ † (Large Col.)	0.25 0.23	Correlation by Ulbrecht et al. (1985) Correlation in Kojima et al. (1980)

*If $U_{og} \propto \bar{\epsilon}$, as determined by Wallis (1969) for churn turbulence.
**Slight effects due to the dependence of voidage, voidage profile exponent, and bubble size on viscosity. In addition, as the liquid viscosity approaches the eddy viscosity, $U_c(0)$ will decrease with viscosity (as shown by Rietema and Ottengraf, 1970).
†This dependence will, in fact, be less due to the change of voidage exponent m with column diameter.

Table 2. Film Reynolds Number

Source	λ	$U_c(\lambda)$ cm/s	$Re_f = \frac{4<U_c(\lambda)>R(1-\lambda)}{\nu_c}$
Small-Column Data ($\ell \propto d$): Hills (1974)			
$U_{og} = 1.9$ cm/s	0.975	−25.9	906
$U_{og} = 3.8$ cm/s	0.977	−37.0	1,184
$U_{og} = 6.4$ cm/s	0.979	−43.0	1,290
Small-Column Data ($\ell \propto d$): Devanathan et al. (1990)			
	0.988	−46.7	1,636
Large-Column Data ($\ell \propto D_c$): Kojima et al. (1980)			
$U_{og} = 2.2$ cm/s	0.998	−62.05	5,212
$U_{og} = 3.6$ cm/s	0.998	−81.8	7,873
$U_{og} = 4.4$ cm/s	0.998	−107.9	12,996

* $<U_c(\lambda)>$ was linearly approximated as $U_c(\lambda)/2$, and falling film thickness was taken to be $R(1-\lambda)$.

variety of experimental conditions. Estimates for predicting the effects of scale-up were deduced based on the dominant scaling law. This was taken as the length which produced minimum energy dissipation. The initiation of turbulence in the downflowing film of liquid near the wall may be reasonably predicted using the data from wetted-wall columns, where transition to turbulence occurs when $Re_f > 1{,}160$ (Portalski, 1963). Table 2 shows estimated values of this film Reynolds number for the different experiments reported here. It is clear from this that the large column data yield film Reynolds numbers well in excess of the transition value, while small column data give values asymptotically close to the transition value. This suggests that Re_f may be the key in pinpointing turbulence conditions.

Acknowledgment

This research was supported by the National Science Foundation (Grant No. CBT-8820472), and their help is gratefully acknowledged.

Notation

- b = bubble breadth, cm
- d = bubble diameter, cm
- D_c = column diameter, cm
- D_e = molecular diffusion constant, cm^2/s
- E_m = mechanical energy dissipation, W
- F_s = slip force, dyne/cm^3
- g = acceleration due to gravity, cm/s^2
- h = bubble height, cm
- ℓ = mixing length scale, cm
- m = exponent, Eq. 4
- p = pressure, Pa
- Q = volumetric flow, cm^3/s
- r = radial coordinate, cm
- R = column radius, cm
- R_c = Reynolds stress tensor, Pa
- Re_f = film-based Reynolds number, $4Q/(\pi D_c \nu_c)$
- T_c = continuous-phase stress tensor, Pa
- U_c = continuous-phase interstitial velocity, cm/s
- U_{og} = superficial gas velocity, cm/s

Greek letters

- α = aspect ratio, h/b
- β = function defined by Eq. 15a
- γ = function defined by Eq. 16a
- ϵ = gas voidage
- $\bar{\epsilon}$ = mean gas voidage
- λ = position of wall velocity maximum, dimensionless
- μ_c = continuous-phase molecular viscosity, g/cm·s
- ν_c = continuous-phase kinematic viscosity, cm^2/s
- ξ = dimensionless radial coordinate, r/R
- ρ_c = continuous-phase density, g/cm^3
- $\bar{\rho}$ = average density, g/cm^3
- σ = interfacial surface tension, dyne/cm
- τ_c = continuous-phase viscous stress tensor, Pa

Superscript

- * = associated with annular downflowing region

Literature Cited

Anderson, K. G., and R. G. Rice, "Local Turbulence Model for Predicting Circulation Rates in Bubble Columns," *AIChE J.*, **35** 514 (1989).

Clark, N. N., C. M. Atkinson, and R. L. C. Flemmer, "Turbulent Circulation in Bubble Columns," *AIChE J.*, **33**, 515 (1987).

Christi, M. Y., B. Halard, and M. Moo-Young, "Liquid Circulation in Airlift Reactors," *Chem. Eng. Sci.*, **43**, 451 (1988).

Cohen, R. D., "Effect of Turbulence Damping on the Steady-State Drop Size Distribution in Stirred Liquid-Liquid Dispersions," *Ind. Eng. Chem. Res.*, **30**, 277 (1991).

Devanathan, N., D. Moslemian, and M. P. Dudukovic, "Flow Mapping in Bubble Columns Using CARPT," *Chem. Eng. Sci.*, **45**(8), 2285 (1990).

Devanathan, N., personal communication (1990).

Fan, L.-S., and K. Tsuchiya, *Bubble Wake Dynamics in Liquid and Liquid-Solid Suspensions*, Butterworth-Heinemann (1990).

Geary, N. W., and R. G. Rice, "Circulation in Bubble Columns: Corrections for Distorted Bubble Shape," *AIChE J.*, **37**, 1593 (1991).

Hills, J. H., "Radial Nonuniformity of Velocity and Voidage in a Bubble Column," *Trans. Int. Chem. Eng.*, **52**, 1 (1974).

Hinze, J. O., *Turbulence*, McGraw-Hill, New York (1975).

Ishii, M., *Thermo-Fluid Dynamic Theory of Two-Phase Flow*, Eyrolles, Paris (1975).

Ishii, M., and N. Zuber, "Drag Coefficient and Relative Velocity in Bubbly, Droplet or Particulate Flows," *AIChE J.*, **25**, 843 (1979).

Joshi, J. B., and M. M. Sharma, "A Circulation Cell Model for Bubble Columns," *Trans. Int. Chem. Eng.*, **57**, 244 (1979).

Koide, K., S. Morooka, K. Ueyana, A. Matsuura, F. Yamashita, S. Iwamoto, Y. Kato, H. Inque, M. Shigeta, S. Suzuki, and T. Akekata, "Behavior of Bubbles in Large Scale Bubble Columns," *J. Chem. Eng. Japan*, **12**(2), 98 (1979).

Kojima, E., H. Unno, Y. Sato, T. Chida, H. Imai, K. Endo, I. Inque, J. Kobayashi, H. Kaji, N. Nakanishi, and K. Yamamoto, "Liquid-Phase Velocity in a 5.5-m-Diameter Bubble Column," *J. Chem. Eng. Japan*, **13**(1), 16 (1980).

Lubbert, A., and B. Larson, "Detailed Investigations of the Multiphase Flow in Airlift Tower Loop Reactors," *Chem. Eng. Sci.*, **45**, 3047 (1990).

Lubbert, A., B. Larson, and S. Broring, "Local Mixing Behaviour of Airlift Multiphase Chemical Reactors," *Int. Chem. Eng. Symp. Ser.*, 121 (1990).

Portalski, S., "Studies of Falling Liquid Film Flow," *Chem. Eng. Sci.*, **18**, 787 (1963).

Prince, M. J., and H. W. Blanch, "Bubble Coalescence and Break-Up in Air Sparged Bubble Columns," *AIChE J.*, **36**, 1485 (1990).

Rice, R. G., and N. W. Geary, "Prediction of Liquid Circulation in Viscous Bubble Columns," *AIChE J.*, **36**, 1339 (1990).

Rietema, K., "Science and Technology of Dispersed Two-Phase Systems: I and II," *Chem. Eng. Sci.*, **37**, 1125 (1982).

Rietema, K., and S. P. P. Ottengraf, "Laminar Liquid Circulation and Bubble Street Formation in a Gas-Liquid System," *Trans. Int. Chem. Eng.*, **48**, T54 (1970).

Schlichting, H., *Boundary Layer Theory*, McGraw-Hill, New York, 568 (1960).

Shah, Y. T., B. G. Kekar, S. P. Godhole, and W. D. Deckwer, "Design Parameter Estimations for Column Reactions," *AIChE J.*, **28**, 353 (1982).

Ulbrecht, J. J., Y. Kawase, and K. F. Auyeung, "More on Mixing of Viscous Liquids in Bubble Columns," *Chem. Eng. Commun.*, **35**, 175 (1985).

Wallis, G. B., *One-Dimensional Two-Phase Flow*, McGraw-Hill, New York (1969).

Walter, J. F., "Bubble Break-Up and Mass Transfer in Gas-Liquid Contactors," Ph.D. Thesis, Univ. of California, Berkeley (1983).

Wisecarver, K. D., Y. T. Shah, and N. Yang, "Phase Behavior in Three Phase Jet Bubble Columns," AIChE Meeting, Paper 181f, Chicago (1990).

Yoshitome, H., and T. Shirai, "The Intensity of Bulk Flow in a Bubble Bed," *J. Chem. Eng. Japan.*, **3**, 29 (1970).

Manuscript received Feb. 11, 1991, and revision received Oct. 28, 1991.